Chemosensitization by Knockdown of Adenine Nucleotide Translocase-2

Morgane Le Bras,[1] Annie Borgne-Sanchez,[2] Zahia Touat,[1] Ossama Sharaf El Dein,[1] Aurélien Deniaud,[1] Evelyne Maillier,[1] Gael Lecellier,[1] Dominique Rebouillat,[2] Christophe Lemaire,[1] Guido Kroemer,[3] Etienne Jacotot,[2] and Catherine Brenner[1]

[1]Centre National de la Reserche Scientifique UMR 8159, Université de Versailles/St. Quentin, Versailles, France; [2]Theraptosis, Pasteur Biotop, Institut Pasteur, Paris, France; [3]Centre National de la Reserche Scientifique UMR 8125, Institute Gustave Roussy, Villejuif, France

Abstract

Mitochondrial membrane permeabilization (MMP) is a rate-limiting step of apoptosis, including in anticancer chemotherapy. Adenine nucleotide translocase (ANT) mediates the exchange of ADP and ATP on the inner mitochondrial membrane in healthy cells. In addition, ANT can cooperate with Bax to form a lethal pore during apoptosis. Humans possess four distinct ANT isoforms, encoded by four genes, whose transcription depends on the cell type, developmental stage, cell proliferation, and hormone status. Here, we show that the *ANT2* gene is up-regulated in several hormone-dependent cancers. Knockdown of ANT2 by RNA interference induced no major changes in the aspect of the mitochondrial network or cell cycle but provoked minor increase in mitochondrial transmembrane potential and reactive oxygen species level and reduced intracellular ATP concentration without affecting glycolysis. At expression and functional levels, ANT2 depletion was not compensated by other ANT isoforms. Most importantly, ANT2, but not ANT1, silencing facilitated MMP induction by lonidamine, a mitochondrion-targeted antitumor compound already used in clinical studies for breast, ovarian, glioma, and lung cancer as well as prostate adenoma. The combination of ANT2 knockdown with lonidamine induced apoptosis irrespective of the Bcl-2 status. These data identify ANT2 as an endogenous inhibitor of MMP and suggest that its selective inhibition could constitute a promising strategy of chemosensitization. (Cancer Res 2006; 66(18): 9143-52)

Introduction

The overall permeability of mitochondrial membranes for metabolites, such as ADP and ATP, results from the permeability of the outer mitochondrial membrane (OM) and that of the inner mitochondrial membrane (IM). In healthy cells, OM permeability is largely dictated by the voltage-dependent anion channel (VDAC), which constitutes a sort of low-specificity molecular sieve allowing for the free diffusion of solutes up to 5,000 Da (1). In comparison, the movement of ions, small molecules, and metabolites must be strictly controlled to allow for the maintenance of the electrochemical gradient on the near-to-impermeant IM. The exchange of ADP and ATP on IM is mediated by a specialized antiporter, the adenine nucleotide translocase (ANT). Several proapoptotic signaling pathways trigger mitochondrial membrane permeabilization (MMP; ref. 2), causing a variable increase in OM and IM permeability. MMP can be induced by proapoptotic members of the Bcl-2 family (e.g., Bax, Bid, and Bnip3; ref. 3), transcription factors (e.g., p53 and Nur77; refs. 4, 5), protein kinases (e.g., Raf and PKCδ; refs. 6, 7), and viral killer proteins (e.g., Vpr from HIV-1 and pB1-F2 from influenza virus; refs. 8, 9) to Ca^{2+} overload (10), oxidative stress (11), and toxic xenobiotics, including some chemotherapeutic agents (for review, see ref. 12). Several antiapoptotic oncoproteins stabilize the permeability barrier of the OM and/or the IM. For instance, Bcl-2 and Bcl-X_L act as MMP inhibitors (13). Stabilization of the OM has been attributed to the Bcl-2/Bcl-X_L-mediated inhibition of local OM-permeabilizing agents, such as VDAC or proapoptotic members of the Bcl-2 family (particularly Bax and Bak; ref. 13). However, how this stabilization is mediated at the level of the IM is an ongoing conundrum.

Previously, we have shown that Bcl-2 can physically interact with ANT. This interaction stimulates the antiporter function of ANT yet inhibits ANT-mediated pore formation (14–16). ANT is an inner membrane protein harboring a physiologic function (i.e., ADP/ATP exchange) and a second proapoptotic function, in which ANT converts into a nonspecific channel (14, 15). The four ANT proteins present in humans (ANT1-ANT4) are encoded by four closely related genes that belong to the mitochondrial carrier family. The ANT isoforms are expressed in a tissue- and development-specific manner (17–19). Reportedly, ANT is a major component of the permeability transition pore (PTP) that can mediate MMP and cell death of cancer cells (for review, see ref. 20). Mitochondria from murine cells lacking both ANT isoforms (ANT1 and ANT2) can still undergo Ca^{2+}-induced swelling (although at a higher threshold; refs. 21, 22), a fact that has been interpreted to mean that ANT is not important for MMP. However, the phenotype of ANT1/ANT2 knockout cells might be explained by functional compensation assumed by the novel isoform identified recently (19) or by other mitochondrial carriers able to form pores in the inner membrane, such as ATP/Mg^{2+} or ornithine/citrulline transporters (for review, see ref. 23). Purified ANT inserted into membranes can form nonspecific pores in response to multiple proapoptotic compounds, including Ca^{2+}, reactive oxygen species (ROS), short chain fatty acids, Bax, Vpr from HIV-1, PB1-F2 from influenza virus, and chemotherapeutic agents, such as verteporfin, MT21 and lonidamine (for reviews, see refs. 20, 24). The pharmacologic inhibition of ANT by protease inhibitor nelfinavir protects mice from three lethal conditions (i.e., CD95/Fas-induced fulminant hepatitis, septic shock, and cerebral ischemia; ref. 25). Accordingly, ANT constitutes a potential therapeutic target (20, 24, 25).

Note: Supplementary data for this article are available at Cancer Research Online (http://cancerres.aacrjournals.org/).

Requests for reprints: Catherine Brenner, Centre National de la Reserche Scientifique UMR 8159, Université de Versailles/St. Quentin, 45 Avenue des Etats-Unis, 78035 Versailles, France. Phone: 33-1-39-25-45-52; Fax: 33-1-39-25-45-72; E-mail: cbrenner@genetique.uvsq.fr.

doi:10.1158/0008-5472.CAN-05-4407

Numerous genes involved in apoptosis are mutated and/or deregulated in cancer cells (26). Bax and Bcl-2, which control MMP, represent a paradigm of apoptosis-related genes whose deregulation contribute to neoplastic cell expansion by suppressing programmed cell death and extending tumor cell life span (27). To date, ANT2 is the only ANT isoform that is overexpressed in tissues with a high level of proliferation, such as liver, lymphocytes (28), and some cancer cell lines (29). As described previously (30, 31), we observed that transfection-enforced overexpression of ANT1 induces apoptosis, whereas ANT2 overexpression has no lethal effect, indicating an isoform-restricted specificity with regard to apoptosis regulation (see Supplementary Fig. S1). Intrigued by this observation, we decided to evaluate the effect of ANT2 on MMP by inactivation of this particular ANT isoform by RNA interference (RNAi). This approach was based on the expectation that ANT2 knockdown may avoid the difficulties inherent to the heterologous overexpression of a membrane protein, which frequently induces an aberrant organelle import, an incorrect folding, and/or altered protein-protein interactions. Here, we report that silencing of ANT2 expression by small interfering RNAs (siRNA) can sensitize tumor cells to apoptotic induction, indicating that ANT2 is an endogenous inhibitor of MMP.

Materials and Methods

When not indicated, products are from Sigma (St. Louis, MO) and cells are obtained from American Type Culture Collection (Rockville, MD).

Cell culture, transfections, and treatments. HeLa-Neo, HeLa-Bcl-2 (human cervix carcinoma; generous gift from V. Goldmacher, ImmunoGen, Cambridge, MA), MCF-7 (human breast adenocarcinoma), HT29 and HCT116 [both human colorectal carcinomas; HCT116 cells were generously given by A. Zweibaum (INSERM, Villejuif, France) and B. Vogelstein, Johns Hopkins University School of Medicine, Baltimore, MD], and HepG2 (human hepatocellular carcinoma) cells were cultured in DMEM supplemented with 10% heat-inactivated FCS and antibiotics at 37°C under 5% CO_2. For transfection, 8×10^4 HeLa-Neo or HeLa-Bcl-2 cells were plated in 24-well plates and then transfected with siRNAs at a final concentration of 50 nmol/L with LipofectAMINE 2000 (Invitrogen, Cergy Pontoise, France) for 5 hours at 37°C. To assess cell drug sensitivity 24 hours after transfection, cells were treated with lonidamine or other therapeutic agents, such as etoposide, arsenite, staurosporine, or the Vpr52-96 peptide, for various periods at 37°C. When indicated, cells were preincubated with rotenone (10 nmol/L), antimycin A (100 nm), or ZVAD (50 μmol/L) before lonidamine treatment.

cDNA cloning and constructs expressing tagged proteins. Total RNA from 293T and HeLa cells was extracted using an RNA isolation kit (RNeasy, Qiagen, Courtaboeuf, France). Following a reverse transcription step using oligo(dT), PCRs were done, with two primers specific for each human ANT isoform [forward primers: 5′-ATGGGTGATCACGCTTGGAGCTTCCTAAAG-3′(hANT1), 5′-ATGACAGATGCCGCTGTGTCCTTCGCCAAG-3′(hANT2), and 5′-ATGACGGAACAGGCCATCTCCTTCGCCAA-3′(hANT3) and reverse primers: 5′-TTAGACATATTTTTTGATCTCATCATACAA-3′ (hANT1), 5′-TTATGTGTACTTCTTGATTTCATCATACAA-3′(hANT2), and 5′-TTAGATCACCTTCTTGAGCTCGTCGTACAG-3′(hANT3)]. Full-length cDNAs encoding each human ANT isoform were then subcloned into pGEM-T vector (Promega, Charbonnieres, France) and sequenced. Recombinant pGEM-T plasmids were used as template in a PCR to generate modified cDNAs using a set of forward primers (containing a *Kpn*I site and an anchor sequence for each isoform) and a set of reverse primers (containing a *Xho*I site and an anchor sequence wherein the STOP codon was replaced by an alanine codon). PCR products were then digested and cloned in the vector pcDNA-V5-3.1 (version A; Invitrogen) into the *Kpn*I and *Xho*I sites. Resulting expression vectors were composed of the open reading frame encoding a human ANT isoform fused to the V5 epitope at its NH_2-terminal part.

RNAi. Oligonucleotides of siRNA were purchased from Proligo (Paris, France). Two duplex sequences were designed for each target gene. siRNA ANT1-1 (nucleotides 127-147): 5′-ACAGAUCAGUGCUGAGAAGdTdT-3′ and 5′-CUUCUCAGCACUGAUCUGUdTdT-3′; siRNA ANT1-2 (nucleotides 461-481): 5′-AUGGUCUGGGCGACUGUAUCAUCdTdT-3′ and 5′-UGAUACAGUCGCCCAGACCAUUCdTdT-3′; siRNA ANT2-1 (nucleotides 127-147): 5′-GCAGAUCACUGCAGAUAAGdTdT-3′ and 5′-CUUAUCUGCAGUGAUCUGCdTdT-3′; and siRNA ANT2-2 (nucleotides 157-177): 5′-GCAUUAUAGACUGCGUGGUdTdT-3′ and 5′-ACCACGCAGUCUAUAAUGCdTdT-3′. Control siRNA molecule was designed as an ANT2 sequence with four mutations: 5′-GCGGAUCGCUACAAAUAAGdTdT-3′ and 5′-CUUAUUUGUAGCGAUCCGCdTdT-3′. As transfection controls, the same double-strand structures were synthesized coupled to fluorescein.

Human ANT isoform-specific primers. To quantify endogenous ANT isoforms in human cell lines by reverse transcription-PCR (RT-PCR), we designed two specific primers for the human ANT isoforms [forward primers: 5′-GCTGATGTGGGCAGGCGCGCCCAGCGTGA-3′ (hANT1), 5′-GCTGATGTGGGTAAAGCTGGAGCTGAAAGGGA-3′ (hANT2), and 5′-GCGGACGTGGGAAAGTCAGGCACAGAGCGC-3′ (hANT3) and reverse primers: 5′-ACAAAAGCACCGCCCATGCCTCT-3′ (hANT1), 5′-ACAAAAGCACCACCCATGCCTCT-3′ (hANT2), and 5′-AGGACGTTGGACCACGCACCC-3′ (hANT3)]. Primer specificity was tested by direct PCR on ANT cDNA and by Northern blot with radiolabeled primers on *in vitro*–transcribed RNA (data not shown).

RNA extraction and RT-PCR. Total RNAs were extracted 24 hours after transfection using the RNeasy Mini kit (Qiagen). After DNase I treatment and enzyme inactivation, the first cDNA strand was synthesized in a mix containing 6 μL RNase-free dH2O, 1 mmol/L dNTPs (Q-BIOgene, Illkirch, France), 4 μL of the 5× buffer, 200 units Mu-MLV RTase (Q-BIOgene), 50 pmol p(dN)25 primers (Q-BIOgene), and 1 μg total RNA, as starting material. The mix was incubated at 37°C for 1 hour followed by 10 minutes at 70°C to denature the reverse transcriptase. PCR was then done in 25 μL final volume containing 3 μL cDNA, 0.4 mmol/L dNTPs, 1 unit Taq DNA polymerase, 2.5 μL of 10× Taq buffer, and 50 pmol of the primer pair specific for each human ANT isoform. The cycle numbers was optimized for each primer pair to detect unsaturated signals (30 rounds of amplification for ANT1 and ANT3 amplification and 26 rounds for ANT2 amplification). For each ANT PCR, we used several specific pairs of primers as internal and loading controls [glyceraldehyde-3-phosphate dehydrogenase (GAPDH) forward, 5′-GGTCGGAGTCAACGGATTTGGTCG-3′, and GAPDH reverse, 5′-CCTCCGACGCCTGCTTCACCAC-3′ and 18S forward, 5′-GTAACCCGTTGAACCCCATT-3′, and 18S reverse, 5′-CCATCCAATCGGTAGTAGCG-3′].

Protein one-dimensional electrophoresis and Western blot. Total proteins were analyzed by SDS-PAGE (12.5% acrylamide gel) and immunoblotting with anti-V5 monoclonal serum (Invitrogen), anti-ANT polyclonal serum (Eurogentec, Searing, Belgium), and anti-tubulin polyclonal serum or anti-Bcl-2 monoclonal antibody (C2 clone, Santa Cruz Biotechnology, Sta Cruz, CA). Proteins were detected by enhanced chemiluminescence (Amersham Pharmacia Biotech, Rockford, IL).

Fluorescence microscopy. For assessment of mitochondrial potential ($\Delta\Psi_m$), cells cultured on coverslips were stained with 100 nmol/L MitoTracker Red CmxRos (Molecular Probes, Cergy Pontoise, France) in complete medium for 15 minutes at 37°C as described previously (32). Necrosis was analyzed by fluorescein diacetate/ethidium bromide (FDA/BET) staining (33). To investigate cytochrome *c* subcellular localization, immunofluorescence was done using a monoclonal-specific antibody (clone 6H2.B4, BD Biosciences, San Jose, CA) followed by a FITC-conjugated anti-mouse antibody (Jackson ImmunoResearch Laboratories, Immunotech SAS, Marseille, France). Cell nuclei were stained with the Hoechst H33342 (2 μmol/L; 15 minutes at 37°C) after three washes with PBS. Then, cells were examined with a fluorescence microscope (DMRHC type, Leica, Rueil-Malmaison, France).

Cytofluorometry. For flow cytometric analysis, HeLa cells were harvested, resuspended in fresh complete DMEM supplemented with appropriate fluorescent probes (100 nmol/L MitoTracker Red CmxRos or 5 μmol/L dihydroethidine; Molecular Probes), and incubated for 15 minutes at 37°C (32). Cell cycle analysis was done as described previously (32).

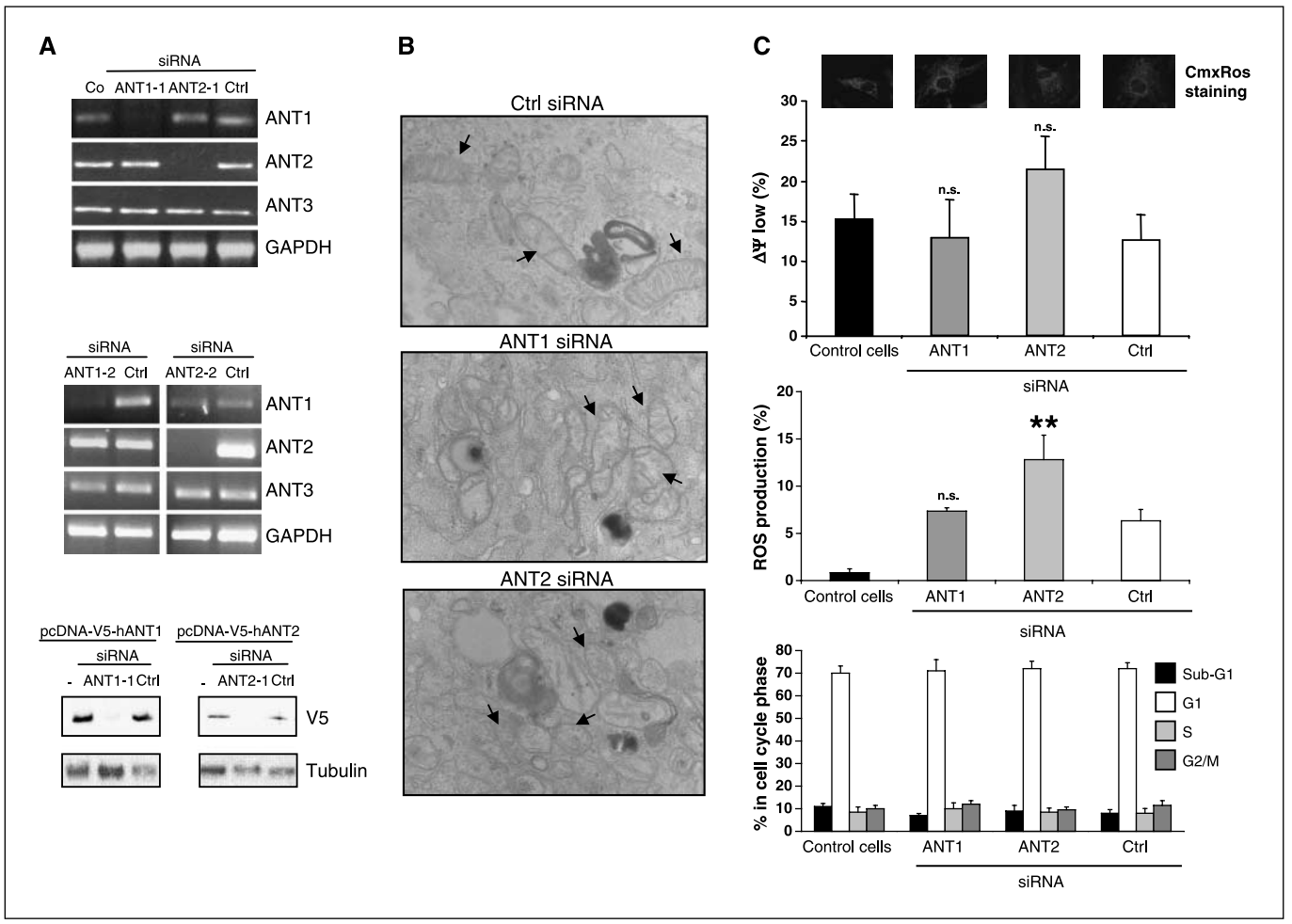

Figure 1. ANT siRNA characterization into HeLa cell line. *A,* specific extinction of endogenous human ANT1 and ANT2 messengers and proteins. HeLa cells were transiently transfected with specific siRNA against human ANT1 or ANT2. Total RNA was extracted and subjected to PCR with specific primer couples for human ANT1, ANT2, or ANT3 and GAPDH as internal control. ANT1-1/ANT1-2 and ANT2-1/ANT2-2 represent different siRNA for ANT1 and ANT2, respectively. To assess siRNA effect on exogenous protein level, HeLa cells were transiently cotransfected with plasmid containing either human ANT1 or ANT2 cDNA, NH_2 terminus tagged with V5 epitope in addition of their corresponding siRNA molecules or control siRNA, and 24 hours later, SDS-PAGE analysis was done and immunoblotted with anti-V5 antibody or anti-tubulin serum. *B,* endogenous ANT extinction does not induce mitochondrial morphologic modifications. Twenty-four hours after transient transfections, HeLa-Neo cells were analyzed for mitochondrial morphology. Electronic microscopy fields presented are representative of a total of 120 mitochondria observed for each condition. *C,* mitochondrial network and membrane $\Delta\Psi_m$ are not or little modified by ANT2 silencing. HeLa cells were transiently transfected with specific siRNA against human ANT1 or ANT2, and 24 hours later, mitochondrial network integrity was investigated by fluorescent microscopy after CmxRos staining and $\Delta\Psi_m$ loss was quantified by flow cytometry on trypsinized and CmxRos-strained cells. ANT2 extinction exerts a slight increase of intracellular ROS level. HeLa cells were transiently transfected with specific siRNA against human ANT1 or ANT2, and 24 hours later, cells were trypsinized and stained with hydroxyethidine to determine cellular O_2^- radicals. Then, labeled cells were counted by flow cytometry. Results are representative of three independent determinations. **, $P = 0.00072$. Cell cycle determination. HeLa cells were transiently transfected with specific siRNA against human ANT1 or ANT2, and 24 hours later, cells were trypsinized, fixed in ethanol, and stained by propidium iodide for DNA content. Repartition into cell cycle phases was determined by flow cytometry. *Columns,* mean of four independent experiments. *n.s.,* nonsignificant.

Transmission electron microscopy. HeLa cells were fixed with 2% glutaraldehyde in 0.1mol/L sodium cacodylate buffer (pH 7.2) for 2.5 hours at 4°C. Samples were then postfixed with 1% osmium tetroxide containing 1.5% potassium cyanoferrate and 2% uranyl acetate in water before gradually dehydrating in ethanol (30-100%) and embedding in Epon resin. Thin sections (80 nm) were collected onto 200 mesh copper grids and counterstained with lead citrate before examination with a Philips CM12 transmission electron microscope (Eindhoven, the Netherlands).

Tissue array analysis. Nylon membrane containing cDNA derived from various human matched normal and tumor tissues or cell lines on Cancer Profiling Array II (Clontech, Palo Alto, CA) was hybridized with ANT2 coding region cDNA fragment labeled with [α-^{32}P]dCTP using Random Primer Labeling kit (Prime-It II, Stratagene, La Jolla, CA), following the manufacturer's instructions. To evaluate the relative expression of *ANT2* gene in these samples, control hybridization was done using ubiquitin given probe as an internal control. Quantification of signals was done using a Molecular Imager system GS-505 (Bio-Rad, Marnes la Coquette, France). ANT2 raw values (normalized on relative ubiquitin abundance) are given in Supplementary Table.

Enzymatic assays. The determination of D-glucose and L-lactic acid amounts in cell culture medium was calculated by UV method, with enzymatic bioanalysis kits from Roche/R-Biopharm (St-Didier au Mont d'or, France), following heat inactivation in the presence of hexokinase, glucose-6-phosphate dehydrogenase, ATP, and NADP according to the manufacturer's instructions. Results were normalized to cellular protein levels.

ADP/ATP exchange. Transfected cells (10^7) were collected and then disrupted in a dounce homogenizor on ice, washed by differential centrifugation (780 × *g* for 10 minutes; 6,000 × *g* for 10 minutes at 4°C) in 5 mmol/L TES, 0.2 mmol/L EGTA, and 0.3 mol/L sucrose buffer (pH 7.2). Total mitochondrial proteins were dosed by microBCA method (Pierce, Palo Alto, CA) and the ADP/ATP exchange rate was then evaluated on

50 μg mitochondrial proteins into a 96-multiwell plate. ATP efflux induced by externally added ADP was monitored by following $NADP^+$ reduction occurring in a buffer containing 2.5 mmol/L glucose, 0.5 E.U. hexokinase (E.C. 2.7.1.1), 0.5 E.U. glucose-6-phosphate-dehydrogenase (Roche/R-Biopharm), and 0.2 mmol/L NADPH (34). The influence of adenylate kinase (ADK)–dependent ATP synthesis was evaluated after treatment of isolated mitochondria with 10 μmol/L ADK-specific inhibitor P_1P_5-diadenosine-5′-pentaphosphate, and no significant effect was observed (data not shown).

ATP quantification. Control or transfected cells were lysed using the lysis solution supplied with the ATP Bioluminescence HS II assay kit (Roche Diagnostics). ATP level in the cell lysates was determined by bioluminescence using a spectrofluorimeter (TECAN GENios, Lyon, France), after oxidation of luciferin in presence of Mg^{2+} and luciferase in accordance with the manufacturer's instructions.

Statistical analysis. Data were analyzed using Student's *t* test for all pairwise comparisons of mean responses among the different treatments tested (SigmaStat software). Results are presented as the mean ± SD for replicate experiments.

Results

ANT1 and ANT2 isoforms are dispensable for cell physiology. We designed two siRNAs specific for ANT1 or ANT2 and transfected them into HeLa cells. After 24 hours of culture, the efficacy of extinction on mRNA expression was confirmed by RT-PCR to be in the range of 80% to 90% (Fig. 1*A*). The siRNAs specific for ANT1 (ANT1-1 and ANT1-2) did not affect the expression of ANT2 (and vice versa, ANT2-1 and ANT2-2), and none of the siRNAs specific for ANT1 or ANT2 affected the abundance of ANT3-specific transcripts (Fig. 1*A*). The specificity of extinction was also analyzed at the protein level in cells expressing epitope-tagged ANT targets. For this, we cotransfected HeLa cells with siRNAs as well as with plasmids expressing human ANT1 or ANT2 carrying the V5 epitope at their NH_2-terminal part. Twenty-four hours later, protein level was analyzed by immunoblotting using anti-V5 antibody. As shown in Fig. 1*A*, ANT1 and ANT2 siRNAs specifically suppressed the expression of V5-hANT1 and V5-hANT2, respectively.

Next, we determined the phenotype of the ANT1 and ANT2 knockdown using for all experiments ANT1-1 and ANT2-1 sequences. Twenty-four hours after transfection, HeLa cells were analyzed by transmission electron microscopy (Fig. 1*B*). Mitochondrial morphology, in terms of number of cristae and matrix condensation, was not affected by siRNA transfection (Fig. 1*B*, *arrows*). The size and number of mitochondria were similar (19 ± 4 mitochondria per 0.1 mm^2). No evidence for mitochondrial swelling, OM rupture, or mitochondria fission could be detected after transfection with control (Fig. 1*B*), ANT1 (Fig. 1*B*), or ANT2 (Fig. 1*B*) siRNAs. More generally, the mitochondrial network seemed to be unaffected by the ANT knockdown by staining with the $\Delta\Psi_m$-sensitive dye CmxRos and fluorescence microscopy analysis (Fig. 1*C*). In parallel, ANT1 knockdown led to a nonsignificant effect on the mitochondrial transmembrane potential ($\Delta\Psi_m$) or ROS level, as determined by CmxRos staining or oxidation of hydroethidine to its fluorescent product ethidium by cytofluorimetric analysis (Fig. 1*C*). In contrast, a low but statistically significant increase in $\Delta\Psi_m$ ($P < 0.01$) and ROS level ($P < 0.001$) was observed in ANT2 siRNA-transfected cells (Fig. 1*C*). ROS might be produced within the mitochondrion because rotenone and antimycin, two inhibitors of the respiratory complex I and III, respectively, decreased significantly their level after ANT2 silencing (Supplementary Fig. S2). All ANT1- or ANT2-specific siRNAs failed to affect the cell cycle phase distribution, with 70 ± 4% of the cellular population being in the G_1 phase, independently of the transfection protocol (Fig. 1*C*).

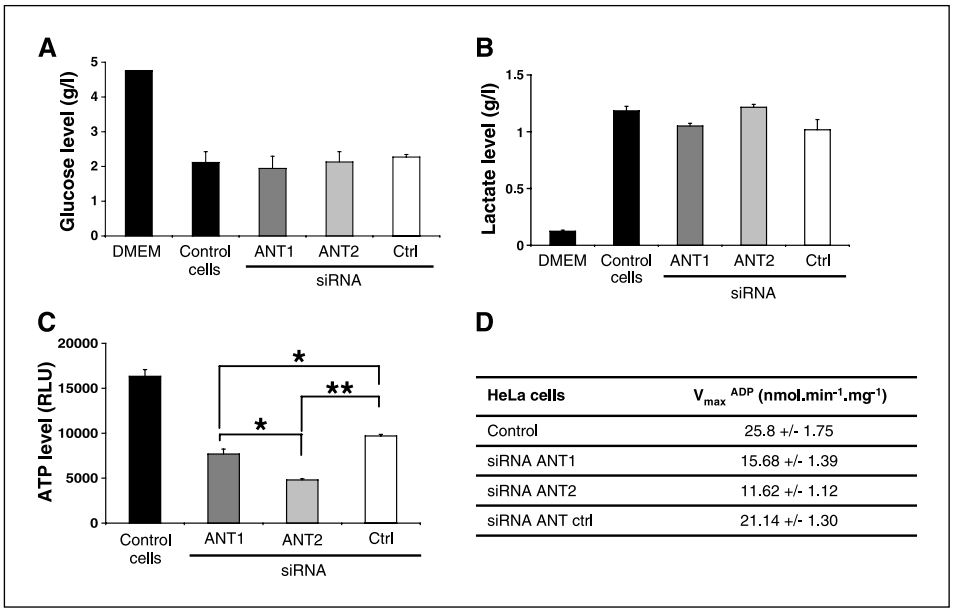

HeLa cells	V_{max}^{ADP} (nmol.min^{-1}.mg^{-1})
Control	25.8 +/- 1.75
siRNA ANT1	15.68 +/- 1.39
siRNA ANT2	11.62 +/- 1.12
siRNA ANT ctrl	21.14 +/- 1.30

Figure 2. ANT2 extinction can alter metabolic variables. *A,* ANT1 or ANT2 extinction modifies glycolysis. HeLa-Neo cells were transiently transfected with specific siRNA against human ANT1 or ANT2, and 24 hours later, cell culture media were collected, heat inactivated, and D-glucose quantified. Results are normalized to total protein level and correspond to three independent measurements. *B,* lactic acid production is not modified when ANT1 or ANT2 isoforms are silenced. Lactic acid was quantified in cell culture medium after 24 hours of contact with HeLa-Neo cells transiently transfected with specific siRNA against human ANT1 or ANT2. Data are normalized to total protein level and correspond to three independent determinations. *C,* ANT2 loss significatively reduces intracellular ATP level. HeLa-Neo cells were transiently transfected with specific siRNA against human ANT1 or ANT2 and lysed 24 hours later for total intracellular ATP quantification. Results expressed in relative luminescence units (*RLU*) are normalized to total protein level and correspond to four independent experiments. *, $P < 0.005$; **, $P < 0.001$. *D,* ANT silencing and ADP/ATP exchange rate. After transient transfection, functional mitochondria from HeLa-Neo cells were isolated and normalized to mitochondrial protein amount and ADP/ATP exchange rate was determined using 500 μmol/L exogenous ADP. Data correspond to three independent determinations.

Altogether, these data indicate that ANT1 or ANT2 depletion can be achieved by specific siRNAs, without major toxic effects that would compromise cellular viability.

ANT extinction induces ATP depletion. As a major carrier in the mitochondrial IM, ANT can modulate cellular metabolic pathways. We tested the consequences of ANT1 and ANT2 extinction on two cellular energetic processes, glycolysis and lactate production. As shown in Fig. 2*A* and *B*, irrespective of which among the two ANT isoforms was knocked down, glucose consumption and lactic acid production remained unaffected. These data confirm that anaerobic glycolysis (and by inference anaerobic ATP production) is not affected by a ANT1 or ANT2 expression. In parallel, we investigated the total intracellular ATP levels after depletion of ANT1 or ANT2. The ANT1-specific siRNA caused an ATP depletion by up to 25% compared with the control siRNA-transfected cells. ANT2 depletion depleted ATP levels by up to 50% (Fig. 2*C*). This strong decrease of global ATP level could be correlated with the ATP/ADP translocation kinetics as measured on mitochondria isolated from ANT1- or ANT2-depleted cells. As summarized in Fig. 2*D*, a significant decrease of ADP/ATP exchange was observed when ANT1 was knocked down (61% of V_{max} measured in controls) and this effect was even more pronounced when ANT2 was silenced (45% of V_{max}). Thus, in HeLa cells, the ADP/ATP translocase function of the two ANT cellular molecules cannot be compensated by other ANT isoforms or by other mitochondrial carriers.

Lonidamine induces the hallmarks of mitochondrial apoptosis that can be potentiated by ANT2 extinction. To further analyze ANT2 silencing effect on chemotherapy-induced apoptosis, we treated ANT2-depleted or control HeLa cells with a panel of cytotoxic agents [i.e., etoposide, an inhibitor of the topoisomerase II; staurosporine, a protein kinase inhibitor; arsenite, a mitochondriotoxic agent; Vpr52-96, a peptide derived from the viral protein targeting ANT; and lonidamine, a derivative of indazole-carboxylic acid that targets mitochondria (35)]. The reduction of the $\Delta\Psi_m$, as determined by CmxRos staining and cytofluorimetric analysis, induced by these compounds was not influenced by ANT2 depletion, except for lonidamine treatment (Fig. 3*A*). Transfection of control siRNA elicited a strong effect on TMP on staurosporine and Vpr treatment and a lower effect on lonidamine, suggesting a possible preactivation of specific cellular targets for staurosporine and Vpr. Lonidamine is an anticancer compound shown to be safe and efficient in clinical studies on solid tumors and in phase II and III for treatment of ovarian, lung, glioma, and breast cancer (36, 37). We have shown previously that several cancer cell lines can be driven into apoptosis by a direct effect of lonidamine on ANT (35). Intrigued by the lonidamine-sensitizing effect of ANT2 silencing, we evaluated the kinetics of the $\Delta\Psi_m$ dissipation induced by lonidamine in cells treated with ANT1- or ANT2-specific siRNAs. ANT2 depletion accelerated the $\Delta\Psi_m$ loss from 6 to 15 hours compared with controls, but ANT1 depletion had no such effect (Fig. 3*B*). The $\Delta\Psi_m$ loss resulted, at least in part, from a PTP opening and was not affected by ANT1 or ANT2 knockdown as measured by calcein staining, a specific labeling method for the PTP opening detection in cellula (refs. 38, 39; data not shown). To further explore the synergistic cytotoxic effects of lonidamine added to ANT2 depletion, we measured additional variables indicative for apoptosis (i.e., production of ROS, cytochrome *c* localization, caspase activation, and loss of nuclear DNA, which causes subdiploidy). The results confirmed that ANT2 silencing combined with lonidamine led to increased $\Delta\Psi_m$ loss (Fig. 3*C*, *a*),

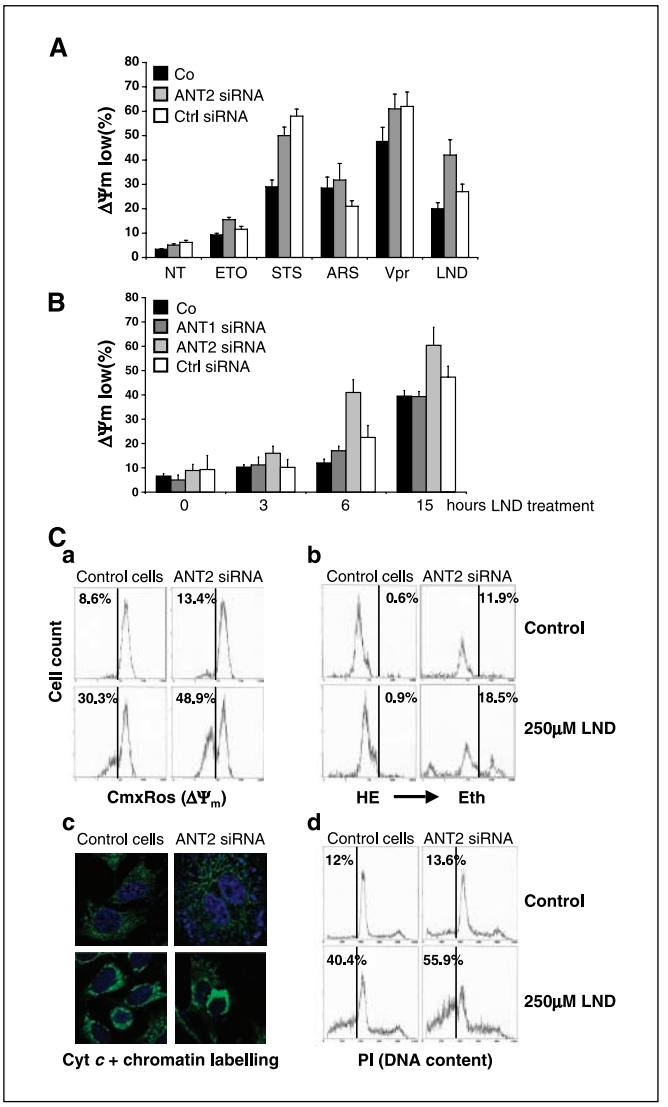

Figure 3. Cellular consequences of specific ANT2 extinction in response to chemotherapeutic treatment. *A,* ANT2 extinction in response to treatment by various chemotherapeutic agents. HeLa-Neo cells were transiently transfected with specific siRNA against human ANT2 (ANT2 siRNA), and 24 hours later, cells were untreated (*Co*) or treated with 100 μmol/L etoposide (*ETO*), 100 nmol/L staurosporine (*STS*), 50 μmol/L arsenite (*ARS*), 1 μmol/L Vpr52-96 (*Vpr*), or 250 μmol/L lonidamine (*LND*) for 6 hours. Then, cells were trypsinized and stained with CmxRos to determine mitochondrial membrane $\Delta\Psi_m$ by flow cytometry. *, $P < 0.01$. *B,* ANT2, but not ANT1, silencing affects mitochondrial membranes in response to lonidamine treatment. HeLa-Neo cells were transiently transfected with specific siRNA against human ANT1 or ANT2, and 24 hours later, cells were untreated or treated with 250 μmol/L lonidamine for various times. Then, cells were trypsinized and stained with CmxRos to measure mitochondrial membrane potential by flow cytometry. *C,* specific ANT2 extinction sensitizes HeLa-Neo cells treated by lonidamine. Apoptotic variables in HeLa-Neo cells transiently transfected with specific siRNA against human ANT2 and untreated or treated with 250 μmol/L lonidamine for 6 hours (or 16 hours before DNA content staining) were analyzed. Excepted for cytochrome c (*Cyt c*) localization determined on coverslips by immunofluorescence (*c*), cells were trypsinized, stained with CmxRos for $\Delta\Psi_m$ measurement (*a*) or hydroxyethidine (*HE*) to measure O_2^- radicals (*b*), or fixed in ethanol (*Eth*) and stained by propidium iodide (*PI*) for DNA content (*d*). Then, cells were counted by flow cytometry. Representative of three independent experiments (*a, b, c*, and *d*).

ROS production (Fig. 3*C, b*), cytosolic cytochrome *c* release (Fig. 3*C, c*), caspase activation (Supplementary Fig. S3), and nuclear DNA loss (Fig. 3*C, e*) compared with cells treated with lonidamine or the ANT2-depleting siRNA alone. Of note, caspase

activation was required for various proapoptotic alterations, including $\Delta\Psi_m$ loss, ROS production, and hypoploidy (Supplementary Fig. S3). Moreover, we observed that plasma membrane permeabilized after the nuclear chromatin condensation correlating again with a death by apoptosis rather than necrosis (data not shown). Thus, 97.6% of dying cells in response to ANT2 extinction and lonidamine treatment died by apoptosis and 2.4% by necrosis as detected by FDA/BET staining (33). We have shown previously that liposomes containing purified rat heart ANT protein (mainly represented by the ANT1 isoform) were permeabilized by lonidamine, in an ATP-inhibitable fashion, whereas plain liposomes remained intact (35). The present data are compatible with the possibility that ANT1 would be the principal target of lonidamine for proapoptotic MMP. Then, the combined modulation of ANT1 (by lonidamine) and ANT2 (by the siRNA) might be particularly toxic.

Cancer-associated alterations in ANT2 isoform expression patterns. To explore the possible implication of the ANT2 isoform in cancer, we determined its expression level in transformed cell lines and tumor samples, notably from lonidamine-sensitive cancers (36). By RT-PCR, we found that ANT2 (but not ANT1) is strongly overexpressed in human cancer cells from various origins compared with normal human fibroblasts and human hepatocytes (Fig. 4*A*). To evaluate the physiopathologic and statistical relevances of these results, we quantified ANT2 in a cohort of patient samples. For this, we used a cancer tissue array, such as normalized cDNA from 154 tumors and adjacent normal tissues from individual patients. The membrane was hybridized with a [α-^{32}P]dCTP-labeled probe corresponding to the entire ANT2 coding region followed by an ubiquitin-specific probe as a loading control (data not shown). As confirmed by Northern blotting on *in vitro* transcripts, the ANT2 probe is isoform specific and did not react with any of the negative controls loaded on the array membrane (data not shown). The relative abundance of ANT2 was assessed in cancer versus normal tissues by phosphoimaging (see Supplemental Table S1). As shown in Fig. 4*B*, ANT2 was significatively overexpressed in cancers developing in breast, ovary, uterus, cervix, thyroid gland, testis, lung, or bladder (see Supplementary Table S1). Of note, human samples with up-regulation of ANT2 expression mainly belong to hormone-sensitive cancers (Fig. 4*B*), which are the same types of cancer reported to up-regulate also cyclophilin D, a matrix protein that reportedly can interact with ANT (40).

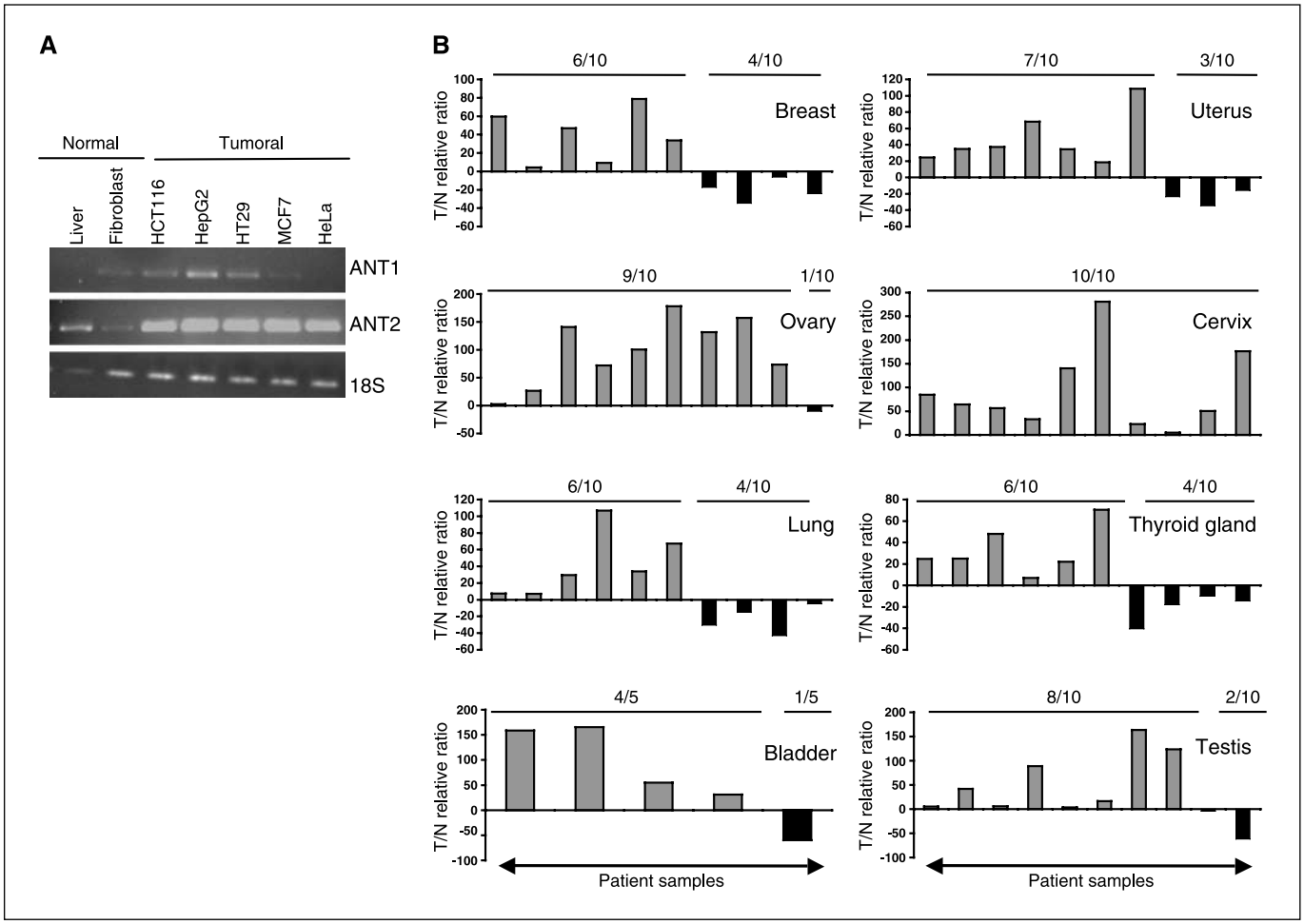

Figure 4. ANT2 expression is dysregulated in cancer. *A,* ANT2 isoform is up-regulated in cancer cell lines. Total RNA was extracted from normal human hepatocytes, fibroblasts, or the indicated tumor cell lines and subjected to RT-PCR analysis of ANT1, ANT2 messengers, or 18S as an internal control. *B,* ANT2 expression is modulated in human cancer tissues. The array containing cDNA from normal tissue (*N*) and tumor tissue (*T*) was hybridized with a radiolabeled probe corresponding to the ANT2 coding region. Relative to the ubiquitin loading control, the tumor tissue/normal tissue ratio is >1 for 60 patient samples, presenting mainly hormone-dependent tumors. *Columns,* one patient. *Gray columns,* patient harboring an increased expression level of ANT2 in tumor tissue versus normal tissue; *black columns,* patient harboring a decreased expression level of ANT2 in tumor tissue versus normal tissue. See Supplementary Table S1 for raw data.

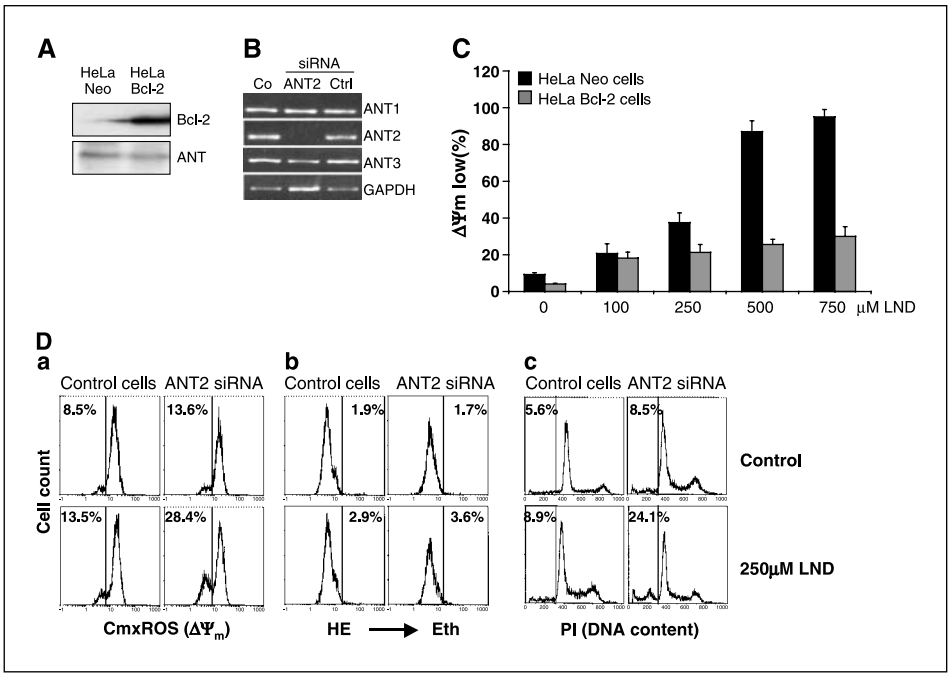

Figure 5. ANT2 extinction overcomes Bcl-2 protection to lonidamine treatment. *A,* Bcl-2 overexpression does not modify ANT expression. Total protein extracts from HeLa-Bcl-2 cells were submitted to SDS-PAGE analysis and immunoblotted with Bcl-2 antibody or polyclonal anti-ANT serum. *B,* specific extinction of endogenous human ANT2 messengers. HeLa-Bcl-2 cells were transiently transfected with specific siRNA against human ANT2. Total RNA was extracted and subjected to RT-PCR with specific primer couples for human ANT1, ANT2, or ANT3 and GAPDH as an internal control. *C,* characterization of dose-independent protection of HeLa-Bcl-2 cells to lonidamine treatment. HeLa-Neo or HeLa-Bcl-2 cells were treated with indicated concentrations of lonidamine for 15 hours. Then, cells were trypsinized and stained with CmxRos. Cells exhibiting a $\Delta\Psi_m$ loss were counted by flow cytometry. *D,* specific ANT2 extinction sensitizes HeLa-Bcl-2 cells treated by lonidamine. Apoptotic variables in HeLa-Bcl-2 cells transiently transfected with specific siRNA against human ANT2 and untreated or treated with 250 μmol/L lonidamine for 6 hours (or 16 hours before DNA content staining) were determined by flow cytometry. Cells were trypsinized, stained with CMxRos for $\Delta\Psi_m$ loss measurement (*a*) or hydroxyethidine to measure O_2^- radicals (*b*), or fixed in ethanol and stained by propidium iodide for DNA content (*c*). Representative experiment repeated thrice (*a, b*, and *c*).

ANT2 extinction overcomes Bcl-2-induced MMP resistance to lonidamine. Bcl-2 overexpression, frequent in cancer, poses a major problem for induction of apoptosis as a curative therapy and is currently targeted for specific inhibition in cancer treatment (41). We investigated whether ANT2 depletion combined with lonidamine treatment might overcome the Bcl-2-mediated chemoresistance. To assess this hypothesis, we transfected HeLa cells stably overexpressing Bcl-2 (Fig. 5*A*) with a siRNA specific for ANT2 (Fig. 5*B*). Of note, expression level of total ANT was not modulated by the stable expression of Bcl-2 (Fig. 5*A*). Although lonidamine alone readily killed HeLa cells transfected with vector only (HeLa-Neo), it failed to induce apoptosis in Bcl-2-transfected HeLa cells (HeLa-Bcl-2; Fig. 5*C*) as shown previously (35). ANT2 depletion combined with lonidamine could induce a $\Delta\Psi_m$ disruption (Fig. 5*D, a*) and a slight but statistically significant increase in hypoploidy (Fig. 5*D, c*) in HeLa-Bcl-2 cells. No evidence of necrosis has been detected, with only 0.8% of HeLa-Bcl-2 cells exerting a necrotic phenotype compared with 28.8% for apoptotic phenotype after ANT2 extinction and lonidamine treatment as detected by FDA/BET staining (33). This chemosensitizing effect was only observed for the ANT2-specific not for the ANT1-specific siRNA (data not shown). Altogether, these results indicate that the down-regulation of ANT2 can overcome the Bcl-2-mediated resistance to lonidamine-induced MMP.

Crosstalk between ANT2, ATP levels, and MMP. Intramitochondrial ATP can be produced by the F_0F_1-ATPase (IM) and the adenylate kinase (matrix and the intermembrane space; ref. 34). Physical interaction between ANT, the Pi carrier, and F_0F_1-ATPase has been observed previously in the liver, where ANT2 is the preponderant isoform (42). This complex, named the ATP synthasome, might be confined to the cristae, whereas ANT1 has been described to be located in the peripheral IM, close to the OM and in interaction with VDAC and cyclophilin D (43, 44). To investigate the functional relationship between cell sensitization to lonidamine exposure and the mitochondrial ATP origin, we measured ATP (Fig. 6*A* and *B*) and $\Delta\Psi_m$ (Fig. 6*C* and *D*) in HeLa-Neo and HeLa-Bcl-2 cells in the absence or presence of oligomycin, a specific inhibitor of the F_0F_1-ATPase.

When added to control cells, oligomycin decreased the intracellular ATP level by 70% (Fig. 6*A*). The combination of ANT1 depletion and oligomycin yielded additive effects. However, oligomycin lost its capacity to deplete ATP following ANT2 knockdown (Fig. 6*A*), presumably because depletion of ANT2 already annihilates the function of the F_0F_1-ATPase function. This corroborates the hypothesis of the ATP synthasome, underscoring that it is the ANT2 isoform and not the ANT1, which is part of this complex. Substantially similar data were obtained for HeLa-Neo (Fig. 6*A*) and HeLa-Bcl-2 (Fig. 6*B*), yet ATP levels were lower in untreated HeLa-Bcl-2 compared with HeLa-Neo.

Because ATP levels can determine whether cells die by apoptosis or by necrosis, we assessed the consequences of oligomycin combined to lonidamine treatment on mitochondrial $\Delta\Psi_m$ of HeLa cells. Oligomycin alone had no detectable effect on $\Delta\Psi_m$, irrespective of whether the ANT1 or ANT2 proteins were depleted from the cells. However, the combination of oligomycin and

lonidamine treatment lead to an enhanced $\Delta\Psi_m$ disruption, except when ANT2 was silenced (Fig. 6*C*). In contrast, in HeLa-Bcl-2 cells, lonidamine and oligomycin exhibited a cooperative toxic effect on $\Delta\Psi_m$, in all the conditions that were assessed, even in ANT2-depeleted cells. This observation is compatible with the fact that Bcl-2 can modulate the pore and translocase functions of ANT (14–16) yet has no effects on the F_0F_1-ATPase (Fig. 6*D*).

Discussion

Human ANT isoforms share important sequence homologies (i.e., 88% identity; ref. 18), but little is known about their differential biological role. Several converging studies suggested that the ANT2 isoform is not proapoptotic (30, 31) and might restore a deficient mitochondrial energetic metabolism of cancer cells by importing ATP within the organelle (45) and therefore might contribute to carcinogenesis. The present study reveals that *ANT2* gene silencing induces a reduction in ATP levels and in the kinetics of ADP/ATP exchange on the IM (Fig. 2). These reductions are consistent with the observation that an isoform shift can alter the kinetic properties of the carrier and can contribute to the disturbance of the energy metabolism *in vivo* (46). In addition, knockdown ANT2 induced an increase of $\Delta\Psi_m$ and ROS level in HeLa cells (Fig. 1), meaning that ANT1 is not able to rescue ANT2 depletion at the level of the oxidative phosphorylation function. One explanation would be that ANT1 is almost inactive in these cells (whereas it is still normally expressed). On glucose-supplemented medium, cells synthesize ATP almost through glycolysis, whereas the OXPHOS activity remains relatively low. Thus, as shown by Faustin et al. (44), a large part of ANT1 could be present as inactive monomeric form unable to restore a normal OXPHOS efficiency. However, all effects cannot be solely attributed to a reduced ATP export from mitochondria because ANT2-depleted cells become refractory to the inhibitory effect of oligomycin (Fig. 6), suggesting that the F_0F_1-ATPase is already inhibited when ANT2 is knocked down. Therefore, our findings clearly support the functional cooperation between ANT2 and F_0F_1-ATPase within the ATP synthasome.

In addition, we found that ANT2 depletion and lonidamine mediated a synergistic proapoptotic response (Fig. 3), even in Bcl-2 overexpressing cells (Fig. 5). Our results suggest that Bcl-2 protection should require a minimal level of ROS in cancer cells. This was already proposed by Clement, et al. (47), who showed that the decrease of intracellular superoxide anion modulates the intracellular pH, caspase 8 activation and favors the extrinsic pathway of cell death. Moreover, a synergistic cell death induction was also observed for the combination of oligomycin and lonidamine, including in Bcl-2-overexpressing cells (Fig. 6). This suggests that lonidamine, when combined with either of two treatments affecting the ATP synthasome (i.e., inhibition of ANT2 by RNAi or pharmacologic inhibition of the F_0F_1-ATPase), causes a major ATP depletion that becomes incompatible with cell survival, irrespective of the Bcl-2 status. Accordingly, one possible mechanism would be the derepression/activation of proapoptotic proteins, which activity is inhibited by ADP or ATP in normal conditions, such as PTP complex or ANT. Thus, ATP is a direct inhibitor of the pore function of ANT, presumably by favoring the so-called matricial conformation (48). Another possible mechanism would be a differential interaction of ANT isoforms with Bax, one of the most important inducer of MMP (12). However, using stable cell lines overexpressing human ANT1 or ANT2, we failed to detect any selectivity in the ANT/Bax interaction (data not shown). Thus, the consequences of the ANT2 knockdown strategy are the decrease in ATP levels and the ATP-dependent sensitization of ANT1 to pore conversion by lonidamine, and when associated, both processes lead to an increase in apoptotic induction.

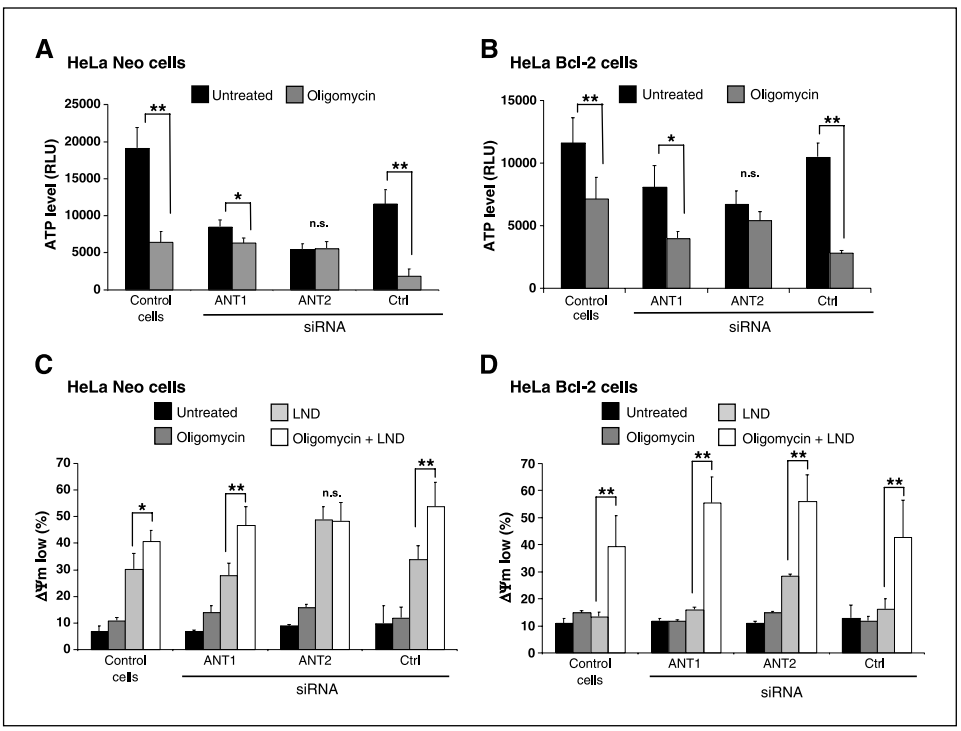

Figure 6. Crosstalk between ATP level and cell sensitivity to lonidamine. *A* and *B*, functional interference of ANT2 and F_0F_1-ATPase in ATP production. HeLa-Neo (*A*) or Bcl-2 (*B*) cells were transiently transfected with specific siRNA against human ANT1 or ANT2 and, 24 hours later, untreated or treated with 2.5 μmol/L oligomycin for 6 hours and lysed according to the manufacturer's instructions. Then, total intracellular ATP was quantified by luminescence. Results expressed in relative luminescence units are normalized to total protein level and correspond to three independent experiments. *, $P < 0.01$; **, $P < 0.001$. *C* and *D*, correlation between ATP level and mitochondrial membrane $\Delta\Psi_m$ loss. HeLa-Neo (*C*) or Bcl-2 (*D*) cells were transiently transfected with specific siRNA against human ANT1 or ANT2, and 24 hours later, cells were left untreated or treated with 2.5 μmol/L oligomycin and/or 250 μmol/L lonidamine for 6 hours. In case of associated treatment, same dose of oligomycin was added for 45 minutes before lonidamine treatment. Then, cells were trypsinized and stained with CmxRos to measure $\Delta\Psi_m$ by flow cytometry. Data are the mean of three independent determinations. *, $P < 0.005$; **, $P < 0.001$.

We found that ANT2 is differentially expressed in human tumor cells (Fig. 4) and notably up-regulated in several hormone-dependent cancers. Interestingly, they correspond to lonidamine-treated tumors in clinical assays, suggesting that ANT2 depletion might increase the efficacy of lonidamine for chemotherapeutic induction of apoptosis in these cancer cells. Moreover, as a result, the expression variation levels were remarkably elevated (>30%) and concerned a high proportion of tumors for each cancer (e.g., 100% of patients for cervix cancer and 90% for ovary cancer; Fig. 4).

The effects of ANT2 knockdown on ATP levels, $\Delta\Psi_m$, ROS, and lonidamine efficacy were not compensated by other ANT isoforms nor other mitochondrial carrier (Figs. 1-3). This corroborates the previous observations on the differential role of ANT isoforms in apoptotic induction, which indicate that heterologous overexpression of ANT1 and ANT3, but not ANT2, can trigger apoptosis in a variety of cancer cells (30), putatively via the mitochondrial recruitment of nuclear factor-κB (31, 49). Due to the high sequence homologies between the various ANT and the conformational homologies between mitochondrial carriers (23), it is tempting to postulate that the differences observed between ANT1 or ANT2 functions might result of different interactions with mitochondrial proteins, such as the F_0F_1-ATPase or VDAC as well as different subcompartmentation in the IM.

Irrespective of these mechanistic considerations, the data presented in this article suggest that ANT2 silencing, combined with a mitochondria-targeted chemotherapy, could constitute a promising approach to enhance apoptotic cancer cell death.

Acknowledgments

Received 12/12/2005; revised 5/10/2006; accepted 7/7/2006.

Grant support: Association pour la Recherche Contre le Cancer, Centre National de la Reserche Scientifique (CNRS), and Ministère délégué à la Recherche et aux Nouvelles Technologies (GenHomme Programs 2001 and 2003) grants N°01H0480 and N°03L297 (C. Brenner) and N°01H0476 and N°03L292 (E. Jacotot); Agence Nationale pour la Valorisation de la Recherche grants N°R0209333Q and N°A0404096Q (E. Jacotot) and N°K0109377Q (D. Rebouillat); European Union grant (G. Kroemer); CNRS Postdoctoral Fellowship (M. Le Bras); and Ligue contre le Cancer Ph.D. Fellowship (A. Deniaud).

The costs of publication of this article were defrayed in part by the payment of page charges. This article must therefore be hereby marked *advertisement* in accordance with 18 U.S.C. Section 1734 solely to indicate this fact.

We thank C. Longin (platform MIMA2, http://voxel.jouy.inra.fr/mima2) for its professional assistance in electron microsocopy.

References

1. Rostovtseva T, Tan W, Colombini M. On the role of VDAC in apoptosis: fact and fiction. J Bioenerg Biomembr 2005;37:129–42.
2. Brenner C, Kroemer G. Apoptosis: mitochondria—the death signal integrators. Science 2000;289:1150–1.
3. Kluck RM, Esposti MD, Perkins G, et al. The pro-apoptotic proteins, Bid and Bax, cause a limited permeabilization of the mitochondrial outer membrane that is enhanced by cytosol. J Cell Biol 1999;147:809–22.
4. Chipuk JE, Kuwana T, Bouchier-Hayes L, et al. Direct activation of Bax by p53 mediates mitochondrial membrane permeabilization and apoptosis. Science 2004;303:1010–4.
5. Li H, Kolluri SK, Gu J, et al. Cytochrome *c* release and apoptosis induced by mitochondrial targeting of nuclear orphan receptor TR3. Science 2000;289:1159–64.
6. Wang H-G, Rapp UR, Reed JC. Bcl-2 targets the protein kinase Raf-1 to mitochondria. Cell 1996;87:629–38.
7. Majumder PK, Pandey P, Sun X, et al. Mitochondrial translocation of protein kinase Cδ in phorbolester-induced cytochrome *c* release and apoptosis. J Biol Chem 2000;275:21793–6.
8. Jacotot E, Ravagnan L, Loeffler M, et al. The HIV viral protein R induces apoptosis via a direct effect on the mitochondrial permeability transition pore. J Exp Med 2000;191:33–46.
9. Zamarin D, Garcia-Sastre A, Xiao X, Wang R, Palese P. Influenza virus PB1-2 protein induces cell death through mitochondrial ANT3 and VDAC1. PLoS Pathog 2005;1:e4.
10. Chakraborti T, Mondal M, Roychoudhury S, Chakraborti S. Oxidant, mitochondria, and calcium: an overview. Cell Signal 1999;11:77–85.
11. Le Bras M, Clement MV, Pervaiz S, Brenner C. Reactive oxygen species and the mitochondrial signaling pathway of cell death. Histol Histopathol 2005;20:205–20.
12. Green DR, Kroemer G. The pathophysiology of mitochondrial cell death. Science 2004;305:626–9.
13. Danial NN, Korsmeyer SJ. Cell death: critical control points. Cell 2004;116:205–19.
14. Marzo I, Brenner C, Zamzami N, et al. The permeability transition pore complex: a target for apoptosis regulation by caspases and Bcl-2-related proteins. J Exp Med 1998a;187:1261–71.
15. Marzo I, Brenner C, Zamzami N, et al. Bax and adenine nucleotide translocator cooperate in the mitochondrial control of apoptosis. Science 1998b;281:2027–31.
16. Belzacq A, Vieira H, Verrier F, et al. Bcl-2 and Bax modulate adenine nucleotide translocase activity. Cancer Res 2003;63:541–6.
17. Deniaud A, Le Bras M, Lecellier G, Brenner C, Kroemer G. ANT1. AfCS/Nature molecular pages 2005;doi:10.1038/mp a:000217.000201.
18. Le Bras M, Deniaud A, Lecellier G, Kroemer G, Brenner C. ANT2. AfCS/Nature molecular pages 2005;doi:10.1038/mp a:000216.000201.
19. Dolce V, Scarcia P, Iacopetta D, Palmieri F. A fourth ADP/ATP carrier isoform in man: identification, bacterial expression, functional characterization, and tissue distribution. FEBS Lett 2005;579:633–7.
20. Halestrap AP, Brenner C. The adenine nucleotide translocase: a central component of the mitochondrial permeability transition pore and key player in cell death. Curr Med Chem 2003;10:1507–25.
21. Kokoszka JE, Waymire KG, Levy SE, et al. The ADP/ATP translocator is not essential for the mitochondrial permeability transition pore. Nature 2004;427:461–5.
22. Halestrap AP. Mitochondrial permeability: dual role for the ADP/ATP translocator? Nature 2004;430:1 p following 983.
23. Palmieri F. The mitochondrial transporter family (SLC25): physiological and pathological implications. Pflugers Arch 2004;447:689–709.
24. Belzacq AS, Brenner C. The adenine nucleotide translocator: a new potential chemotherapeutic target. Curr Drug Targets 2003;4:517–24.
25. Weaver JGR, Tarze A, Moffat TC, et al. Inhibition of adenine nucleotide translocator pore function and protection against apoptosis *in vivo* by an HIV protease inhibitor. J Clin Inves 2005;115:1828–38.
26. Hanahan D, Weinberg RA. The hallmarks of cancer. Cell 2000;100:57–70.
27. Reed J. Bcl-2 family proteins. Oncogene 1998;17:3225–36.
28. Giraud S, Bonod-Bidaud C, Wesolowski-Louvel M, Stepien G. Expression of human ANT2 gene in highly proliferative cells: GRBOX, a new transcriptional element, is involved in the regulation of glycolytic ATP import into mitochondria. J Mol Biol 1998;281:409–18.
29. Lunardi J, Attardi G. Differential regulation of expression of the multiple ADP/ATP translocase genes in human cells. J Biol Chem 1991;266:16534–40.
30. Bauer MK, Schubert A, Rocks O, Grimm S. Adenine nucleotide translocase-1, a component of the permeability transition pore, can dominantly induce apoptosis. J Cell Biol 1999;147:1493–502.
31. Zamora M, Granell M, Mampel T, Vinas O. Adenine nucleotide translocase 3 (ANT3) overexpression induces apoptosis in cultured cells. FEBS Lett 2004;563:155–60.
32. Jan G, Belzacq AS, Haouzi D, et al. Propionibacteria induce apoptosis of colorectal carcinoma cells via short-chain fatty acids acting on mitochondria. Cell Death Differ 2002;9:179–88.
33. Lemaire C, Andreau K, Souvannavong V, Adam A. Inhibition of caspase activity induces a switch from apoptosis to necrosis. FEBS Lett 1998;425:266–70.
34. Passarella S, Ostuni A, Atlante A, Quagliariello E. Increase in the ADP/ATP exchange in rat liver mitochondria irradiated *in vitro* by helium-neon laser. Biochem Biophys Res Commun 1988;156:978–86.
35. Belzacq AS, El Hamel C, Vieira HL, et al. Adenine nucleotide translocator mediates the mitochondrial membrane permeabilization induced by lonidamine, arsenite, and CD437. Oncogene 2001;20:7579–87.
36. Di Cosimo S, Ferretti G, Papaldo P, Carlini P, Fabi A, Cognetti F. Lonidamine: efficacy and safety in clinical trials for the treatment of solid tumors. Drugs Today 2003;39:157–74.
37. Oudard S, Carpentier A, Banu E, et al. Phase II study of lonidamine and diazepam in the treatment of recurrent glioblastoma multiforme. J Neurooncol 2003;63:81–6.
38. Petronilli V, Miotto G, Canton M, et al. Transient and long-lasting openings of the mitochondrial permeability transition pore can be monitored directly in intact cells by changes in mitochondrial calcein fluorescence. Biophys J 1999;76:725–34.
39. Lemasters J, Nieminen A, Qian T, Trost L, Herman B. The mitochondrial permeability transition in toxic, hypoxic, and reperfusion injury. Mol Cell Biochem 1997;174:159–65.
40. Schubert A, Grimm S. Cyclophilin D, a component of the permeability transition-pore, is an apoptosis repressor. Cancer Res 2004;64:85–93.
41. Bouchier-Hayes L, Lartigue L, Newmeyer DD. Mitochondria: pharmacological manipulation of cell death. J Clin Invest 2005;115:2640–7.
42. Ko Y, Delannoy M, Hullihen J, Chiu W, Pedersen P. Mitochondrial ATP synthasome. Cristae-enriched membranes and a multiwell detergent screening assay yield dispersed single complexes containing the ATP synthase and carriers for Pi and ADP/ATP. J Biol Chem 2003;278:12305–9.

43. Vyssokikh MY, Katz A, Rueck A, et al. Adenine nucleotide translocator isoforms 1 and 2 are differently distributed in the mitochondrial inner membrane and have distinct affinities to cyclophilin D. Biochem J 2001; 358:349–58.
44. Faustin B, Rossignol R, Rocher C, Benard G, Malgat M, Letellier T. Mobilization of adenine nucleotide translocators as molecular bases of the biochemical threshold effect observed in mitochondrial diseases. J Biol Chem 2004;279:20411–21.
45. Malthiery Y, Stepien G. ANT2 expression under hypoxic conditions produces opposite cell-cycle behavior in 143B and HepG2 cancer cells. Mol Carcinog 2005; 42:1–8.
46. Dorner A, Giessen S, Gaub R, et al. An isoform shift in the cardiac adenine nucleotide translocase expression alters the kinetic properties of the carrier in dilated cardiomyopathy. Eur J Heart Fail 2005;8:81–9.
47. Clement MV, Hirpara JL, Pervaiz S. Decrease in intracellular superoxide sensitizes Bcl-2-overexpressing tumor cells to receptor and drug-induced apoptosis independent of the mitochondria. Cell Death Differ 2003;10:1273–85.
48. Belzacq AS, Vieira HL, Verrier F, et al. Bcl-2 and Bax modulate adenine nucleotide translocase activity. Cancer Res 2003;63:541–6.
49. Zamora M, Merono C, Vinas O, Mampel T. Recruitment of NF-κB into mitochondria is involved in adenine nucleotide translocase 1 (ANT1)-induced apoptosis. J Biol Chem 2004;279:38415–23.

Chemosensitization by Knockdown of Adenine Nucleotide Translocase-2

Morgane Le Bras, Annie Borgne-Sanchez, Zahia Touat, et al.

Cancer Res 2006;66:9143-9152.